This article has been accepted for publication in IEEE Transactions on Dielectrics and Electrical Insulation. This is the author's version which has not been fully edited and content may change prior to final publication. Citation information: DOI 10.1109/TDEI.2024.3445873

Correlation Analysis between Discharge Image Characteristics and Current of the Rod-plate Gap under Lightning Impulse

Yaqi Zhang, Ziqiang Cai, Yongxia Han, Gang Liu, Lu Qu, and Licheng Li

***Abstract*—The discharge images with different types could express the discharge process at different angles, which plays an important role in discharge observation. ICCD (Intensified Charge-Coupled Device) image is a key tool for observing and interpreting the fast dynamic discharge process because of the nanosecond scale exposure duration. There are still few analyses of the low-level features in ICCD images of meter-level gap discharge under lightning impulse and research on its correlation with current. Therefore, based on the Electron Multiplying ICCD, repetitive discharge experiments of the 1 m rod-plate air gap under standard lightning impulse were carried out. Synchronous discharge intensity images with nanosecond exposure time and time interval, discharge current and voltage were collected. Combined with the analysis of image characteristics and discharge mechanism, the correlation between the longitudinal average light intensity along the rod-plate axis in images and the discharge current was proposed and verified. And the corresponding empirical formula of two parameters above was given and discussed. By analyzing the correlation between image characteristics and current, it is helpful for achieving a quantifiable description of discharge status and discharge characteristics, and providing new research ideas for discharge space charge distribution and current monitoring methods.**

***Index Terms*—EMICCD image characteristics, discharge current, quantitative correlation, 1 m rod-plate air gap, lightning impulse**

I. Introduction

Discharge study helps to utilize the discharge process and prevent discharge damages. Discharge image is the macroscopic expression of microscopic physical change, which plays an important role in discharge observation. Due to limitations of equipment, early discharge image analysis was qualitative [1-3]. With developing image technology, getting digital images reasonably and mining the hidden information in digital images to describe discharge states and features can help reveal and improve the mechanism of long gap discharge [4]. There are various types of images applied for discharge research including ultraviolet (UV) images [5], infrared images [6], schlieren images [7], visible light images [8], and ICCD (Intensified Charge Coupled Device) images [9]. ICCD image is a key tool to observe the dynamic process of discharge with the nanosecond scale exposure duration. However, it is mainly used in short gap discharge observation for a contradiction between the shooting range of the discharge and the shooting time interval [9-13]. For long gap discharges, ICCD images are used to describe the macroscopic characteristics of the discharge process (morphological characteristics, development speed, discharge stage, etc.). P O Kochkin et al. recorded 1 m air gap discharge images between two conical electrodes under 1.2/50 μs lightning impulse with different exposure times [14, 15]. Ali Shirvani et al. established a new system and observed the streamer and leader discharge processes of the 2-4 m rod-plate air gap discharge under 1.2/50 μs positive lightning impulse. The discharge process was divided into four main stages: first streamer, second streamer, backward wave, and leader. The backward wave is formed by free electrons (or the ionizing wave) starts from the plane-electrode and travels backwards to the anode [16, 17]. And most of such high-level feature [18] (semantic features, such as the shape, bifurcation, velocity, length of the streamer and leader) descriptions are qualitative rather than quantitative.

The discharge current development also shows significant data on the propagation of the voltage breakdown and the time behavior of the current distribution within the discharge plasma. While the measurement of time-resolved discharge current in long gap discharge remains some problems due to the shortcomings of dynamic range and bandwidth [19]. For example, in long gap discharge, there exists the problem of peak clipping or inability to measure weak streamer current because of the relatively small measurement range compared to the change in discharge current. Meanwhile, the discharge current may be disturbed by the electromagnetic interference associated with the applied high voltage [20].

In order to further elucidate the discharge mechanism through multi-angle correlation analysis between discharge

This work was supported in part by Guangzhou Science and Technology Plan (2023A04J0293), and National Engineering Research Center of UHV Technology and Novel Electrical Equipment Basis.

(Corresponding author: Yongxia Han)

Yaqi Zhang and Ziqiang Cai are with Guangdong Polytechnic Normal University, Guangzhou 510665, China (e-mail: zhangyaqimail@126.com; 1434409823@qq.com).

Yongxia Han is with South China University of Technology, Guangzhou 510641, China (e-mail: epyxhan@scut.edu.cn).

Gang Liu and Licheng Li are with Electric Power Research Institute. CSG, Guangzhou 510663, China (e-mail: liugang@csg.cn; qulu@csg.cn; lilc@csg.cn).

This article has been accepted for publication in IEEE Transactions on Dielectrics and Electrical Insulation. This is the author's version which has not been fully edited and content may change prior to final publication. Citation information: DOI 10.1109/TDEI.2024.3445873

images and current, Akif Gürlek observed the discharge development image of a 1.5 m rod-rod gap under an 200 kHz oscillating lightning impulse voltage, and explained its discharge process in conjunction with current changes [21]. Zhao Xiangen et al. analyzed the velocity-current relationship of the positive leader discharge in 3-5 m rod-plate gaps [20]. These literatures reveal the relationship between the high-level features in discharge image and the current. However, there are few research on the relationship between ICCD image low-level features [18] (the underlying feature that reflects image content directly, such as intensity distribution) and discharge current. According to discharge theoretical analysis and principles of ICCD imaging, the ICCD light intensity images could reflect the ionization characteristics during the discharge process. The ionization process of molecules in the gap generates numerous free electrons, forming a discharge current. If the relationship between discharge image characteristics and the current can be explained, it will help us further understand the micro process of discharge and the mechanism of discharge by directly using discharge images. And it could provide new ideas for the study of discharge space charge distribution and current monitoring methods.

Therefore, the aim of this study is to extract the characteristics of the image and analyze the relationship between image characteristics and discharge current in a quantitative manner. Based on the Electron Multiplying ICCD (EMICCD), repetitive discharge experiments of the 1m rod-plate air gap under standard lightning impulse in the indoor impact experimental field of the National Engineering Laboratory of Ultra High Voltage Engineering Technology (Kunming) were performed. By changing EMICCD shutter trigger delay, the discharge intensity images containing the whole gap with nanosecond exposure time and time interval were captured. And through a synchronous trigger system, discharge current and voltage were collected. The changes in the discharge light intensity characteristics were explored on the foundation of the processing and analysis of EMICCD images at different shooting times. The correlation between the longitudinal average light intensity integral and the discharge current was proposed and verified based on discharge theory and experimental analysis. And the corresponding empirical formula of two parameters above was given and discussed.

II. Methods

A. Research strategy

The research strategy diagram was shown in **Fig. 1**. Avoiding environmental light affecting the experimental image results, especially the streamer image with weak discharge, the background noise reduction on the discharge image was performed first. Based on the calculation of shooting time, a series of discharge images were obtained over time. The typical light intensity distribution feature was extracted and discussed. Finally, a hypothesis was proposed based on the principles of current and image formation. The relationship between the current and image characteristics was verified and explained through two sets of data (one set was for discovery, the other was for validation).

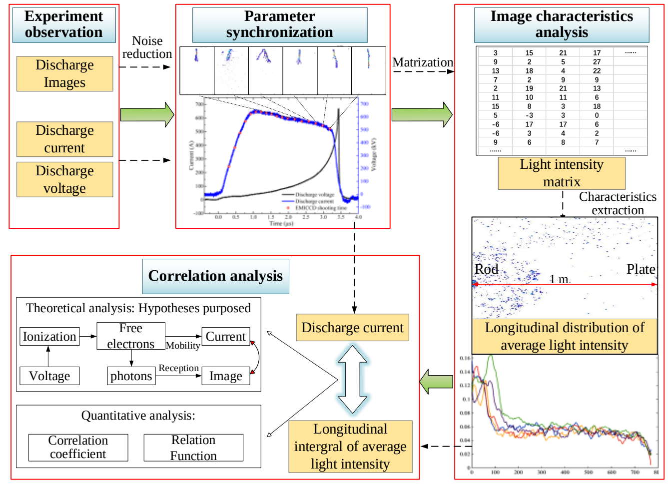

Fig. 1. Research strategy diagram.

B. Discharge observation system

The discharge experiment of a 1m rod-plate gap under the lightning impulse was conducted at the indoor experimental site of the National Engineering Laboratory of UHV Engineering Technology (Kunming) [22] at an altitude of 2100 m. The arrangement of the experimental measurement system with synchronous triggering was shown in **Fig. 2**.

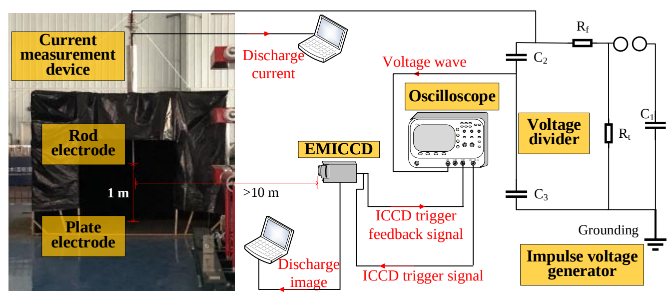

Fig. 2. The arrangement of the experimental measurement system with synchronous triggering.

The experimental equipment mainly included an impulse voltage generator, voltage divider, EMICCD (electron-multiplying intensified charge-coupled device), current measurement device, and oscilloscope. The voltage generator had a rated voltage of 1,600 kV, and a rated capacity of 320 kJ. Its circuit was bilateral high-efficiency, which could generate a standard lightning wave. The highest efficiency was over 90%. EMICCD model was Princeton Instruments PI-MAX4 with high resolution and good linear gain. The lens model, AF-S NIKKOR 24-70MM F/2.8G ED, was used. The current measuring adapted a digital optical method in a long air gap. The coaxial current sensor and a digital optical fiber transmission system were part of the entire current measuring device. The discharge current was evaluated by employing a current sensor that was placed in series with the discharge electrode [19, 23]. The detailed description of the device parameters was mentioned in relative reference [24]. The head of the rod electrode was a hemisphere, with a diameter of 3.75 cm, and the body extended to a length of 30 cm. The plate electrode was composed of a 3×3 m iron plate. The entire gap was located in the darkroom to ensure the experiment safety and the accuracy of the shooting.

The synchronous trigger system with an oscilloscope was designed for EMICCD shooting. The triggering delay set by EMICCD and various transmission line delays (including the signal transmission time from the impulse voltage generated to the oscilloscope receiving this voltage signal, the transmission time from oscilloscope trigger signal EMICCD receiving it, and the transmission time from the EMICCD feedback signal generated to oscilloscope receiving it) should be considered. After a series of transmission delay tests and calculations, the starting time of each discharge image shooting relative to the discharge voltage can be determined.

The experiments were carried out in accordance with the experiment and measurement methods specified in IEC [25, 26]. The indoor temperature was about 22-26 ℃, the relative humidity was 48%-70%, and the air pressure was 789.8-790.1 hPa.

C. Measurement method and content

The system above was used to observe the entire process of the rod-plate gap discharge under 1.2/50 μs positive lightning impulse with a preset voltage level of 616 kV. The observed parameters included discharge voltage, discharge current, and the discharge images at different times.

The discharge voltage was collected by the voltage divider. The time-resolved digital optical measurement device was used to record the discharge current. Considering the limitations on the size of the captured EMICCD continuous image, the discharge images were recorded from repeated discharge at the same impulse voltage level. And only one image containing the entire gap was taken per discharge. By setting different EMICCD triggering delays and light intensity gains, the discharge development in the whole rod-plate gap could be observed over time [24]. The EMICCD trigger delay setting started at 26 ns because of the minimum ICCD trigger delay of 26 ns.

The 10 ns exposure time was set after the EMICCD stability test of the exposure time. The following analysis assumed that the image recorded the transient discharge process at a certain moment during the discharge process because of the extreme exposure time of 10 ns.

The EMICCD light intensity gain was adjusted (the range of 1-500) to observe the extremely weak streamer discharge process and the leader with strong luminescence.

The experiment comprised two groups with consistent impulse voltage and an environment. In the first group of experiments, discharge images in lightning impulse discharge processes were captured with the shorter interval times of 50 or 100 ns. The shooting distance between the EMICCD and the rod-plate gap was about 14 m. In the second group of experiments, for further validation, images of the discharge process were captured with the interval time of 100 or 200 ns. The shooting distance was about 20 m, and the signal transmission lines were longer than those in the first group of experiments.

D. Data filtering and preprocessing

To avoid the impact of discharge dispersion and discharge development randomness on the experimental results, a large number of repetitive discharge process photos were taken, with about 500 effective discharges. The discharge test results with a breakdown time error of less than ±5% from the experiments (3.1-3.4μs) were selected to ensure the similarity in discharge. After the discharge current comparison from multiple tests, the test data with current errors within 10% were filtered for ultimate analysis.

Image denoising was performed in two steps. First, EMICCD was used to capture the background image without discharge before each shooting. So the next captured image will be automatically removed from background noise by EMICCD. And then bilateral filtering method was adapted to further reduce the image noise [27].

III. Experimental Results

The peak of the positive lightning impulse voltage was approximately 651 kV. It was about 20.6% higher than the positive $U_{50\%}$ of the rod-plate gap under 1.2/50 μs lightning impulse. 78 light intensity images were obtained from two sets of rod-plate gap discharge experiments by regularly increasing the EMICCD triggering delay (the first group of experiments: 53 images; the second group of experiments: 25 images).

After noise reduction processing, the series of EMICCD discharge two-dimensional images captured at different times in the first and the second group of experiments were shown in **Fig. 3** and **Fig. 4**. **Fig. 3(a)** presented the synchronized lightning impulse, discharge current, and timing sequences of image shooting in the first groups of experiments. **Fig. 3(b)** presented the corresponding discharge images. **Fig. 4** showed the similar results in the second group of experiments. The light intensity gains in all the images were transformed into 1. The images consisted of 1024×1024 pixels, with the coordinates indicating their positions. The numbers in **Fig. 3(a)** and **Fig. 4(a)** correspond to the number of each image in **Fig. 3(b)** and **Fig. 4(b)**, respectively. Considering the same discharge conditions in two groups of experiments and the smaller errors of discharge data after filtering, the same set of voltage and current data was used in **Fig. 3(a) and Fig. 4(a)** to describe the time correspondence among voltage, current, and images.

It can be seen that the discharge image captured by the above method can reproduce the entire discharge process. Compared to the streamer discharge process (before 0.92 μs), the dispersion of the leader discharge (from 0.92 μs to 3.25 μs) was greater because each discharge image corresponds to a separate discharge process. The discharge images obtained from the two sets of experiments have similar patterns over time. The above analysis indicates that the images obtained in this experiment were reliable.

The images obtained at 2.58 μs still exhibit notable noise even after denoising during the second experiments, making them unsuitable for further image analysis. The decrease in anti-noise ability could be attributed to the longer shooting distance and signal transmission line length. There are a total of 61 valid images for analysis, with 49 images in the first group of experiments and 12 images in the second group.

This article has been accepted for publication in IEEE Transactions on Dielectrics and Electrical Insulation. This is the author's version which has not been fully edited and content may change prior to final publication. Citation information: DOI 10.1109/TDEI.2024.3445873

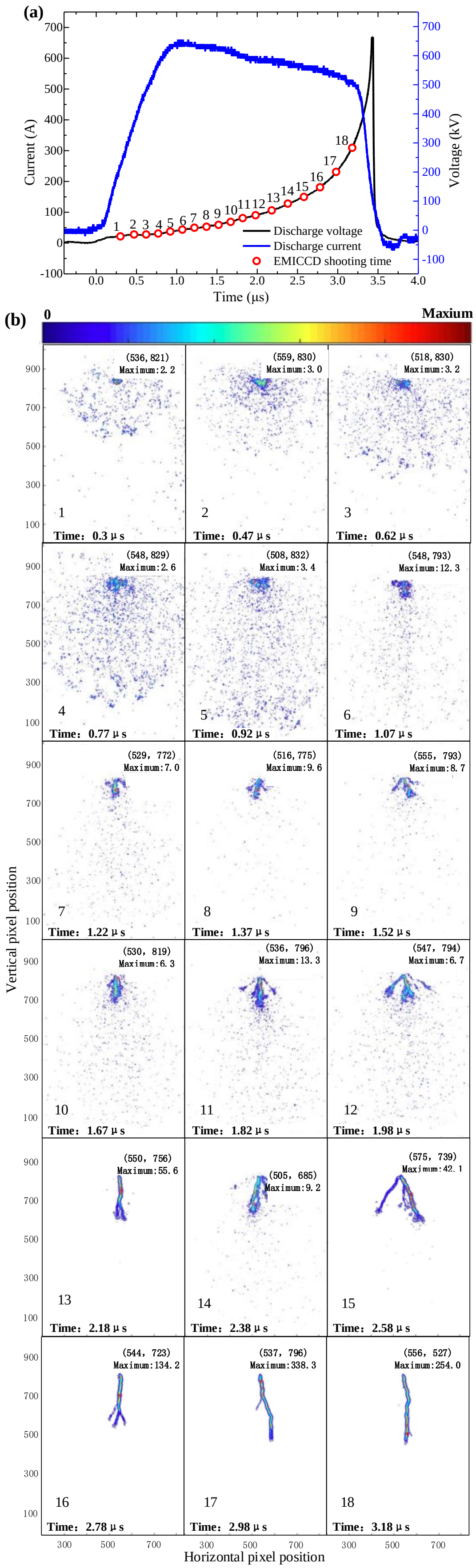

Fig. 3. The typical experimental results in the first group of experiments. (a) the synchronized lightning impulse, discharge current, and timing sequences of image shooting. (b) the corresponding discharge images over time.

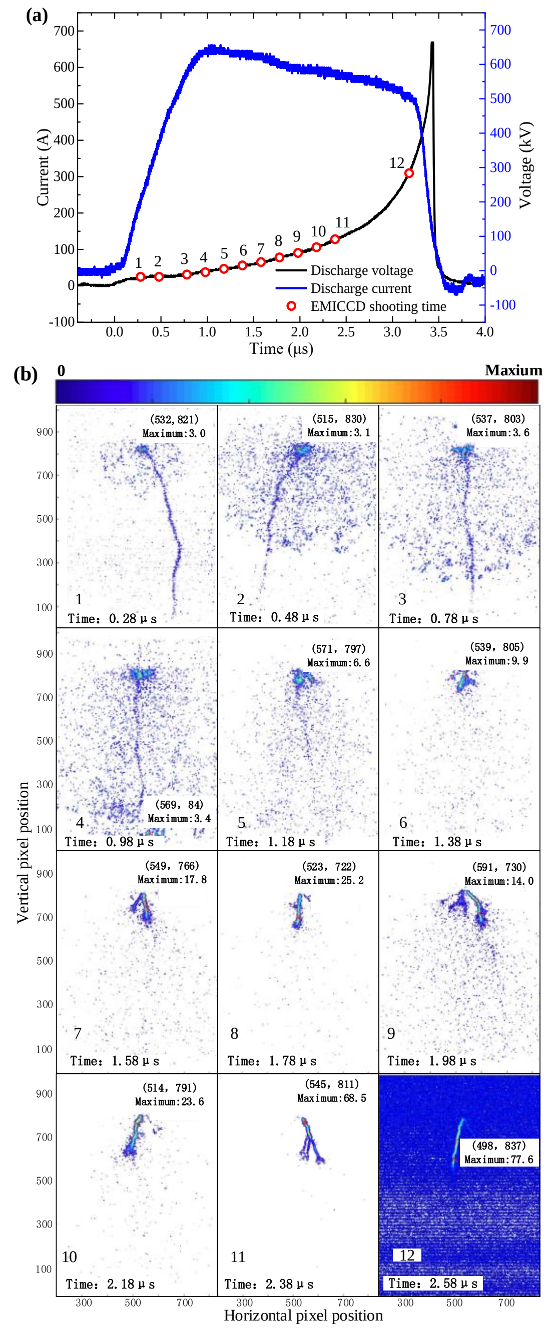

Fig. 4. The typical experimental results in the second group of experiments. (a) the synchronized lightning impulse, discharge current, and timing sequences of image shooting. (b) the corresponding discharge images over time.

IV. ANALYSIS OF RESULTS

This article has been accepted for publication in IEEE Transactions on Dielectrics and Electrical Insulation. This is the author's version which has not been fully edited and content may change prior to final publication. Citation information: DOI 10.1109/TDEI.2024.3445873

A. Image characteristics

Further analysis of the light intensity characteristics is performed based on the obtained discharge images in the first group of experiments. During the discharge ionization process, a portion of the energy will be emitted as photons. EMICCD received the photons in different areas and formed the discharge image. As shown in **Fig. 5** the shooting time of the light intensity image is 0.3 μs. The real gap distance is 1 m located between 50 and 820 vertical pixels in the image. The actual length for each pixel point can be calculated to be 0.13 cm. Since the discharge process develops from the rod electrode to the plate electrode, the longitudinal variation of light intensity along the rod-plate axis is explored. To avoid errors in light intensity analysis at few pixel positions, the image data within the range of 520 ± 420 pixels on the horizontal axis (included the entire discharge ionization region) is considered.

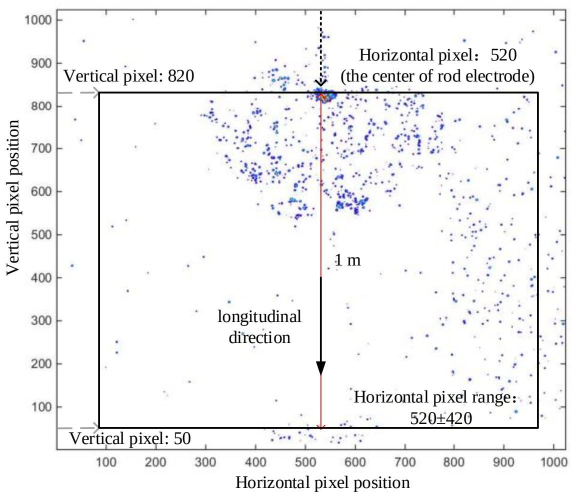

Fig. 5. Schematic diagram of image analysis.

Analysis of longitudinal average light intensity distribution in the rod-plate gap is conducted. The horizontal coordinate of the center position of the rod electrode is 520. The longitudinal distributions of the average light intensity at different discharge times are shown in **Fig. 6**.

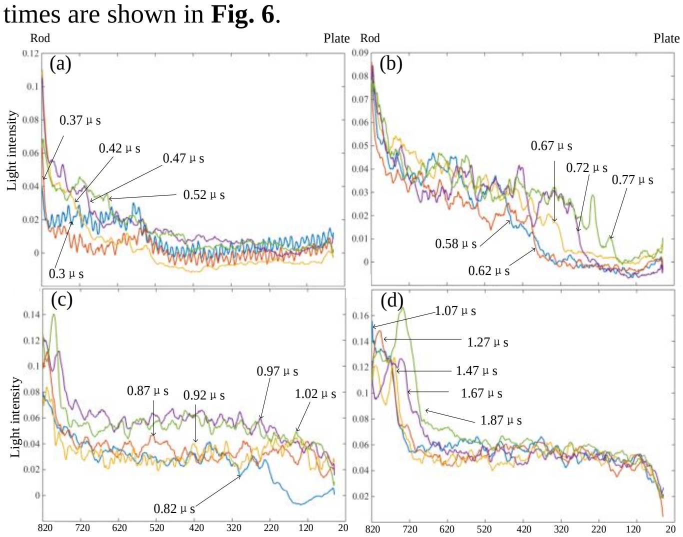

Fig. 6. The longitudinal distribution differences of the average light intensity in chronological order. (a) the average light intensity distribution during 0.3-0.52 μs with interval time 40-50 ns. (b) the average light intensity distribution during 0.58-0.88 μs with interval time about 40-50 ns. (c) the average light intensity distribution during 0.82-1.02 μs with interval time 50 ns. (d) the average light intensity distribution during 1.07-1.87 μs with interval time 200 ns.

It can be seen in **Fig. 6** that the light intensity at the head of the rod is stronger than other positions, and the light intensity at other positions is weaker, but a few of the maximum light intensity values will appear in the middle. There is an obvious trend of the position of the maximum light intensity moving towards the plate over time during the streamer development (before 0.92 μs). When the leader developing, the maximum light intensity at the head of the rod moves towards the plate over time. These trends bear resemblance to the change in electron density along the axial direction in rod-plate gap discharge, providing evidence for the significant link between discharge light intensity, ionization, and electron movement.

B. The correlation between discharge current and image characteristics

Under the lightning impulse, the ionization process produced by a strong electric field develops rapidly in the rod-plate gap. The discharge current near the rod electrode is the vector sum of electron and ion currents generated by discharge ionization. The free electrons formed by strong ionization have high kinetic energy and are in the excited state. When the excited state electrons transition back to the ground state (the electrons in the atom transition from the high energy level to the low energy level), the energy released can be expressed as heat energy, photon, etc.

The light intensity images can reveal two aspects of ionization characteristics during the discharge process, based on the principle of light intensity image formation and discharge mechanism. One is the discharge ionization position (image coordinates), and the other is the degree of ionization at a certain position (light intensity). The ionization process of molecules in the gap (collision ionization, photoionization, thermoelectric ionization, etc.) will cause a large number of free electrons. The movement of free electrons handles the discharge current (with the movement of ions being disregarded in rapid discharge).

Hence, by assuming a correlation between current and light intensity, we compare the average light intensity integration at different times with the discharge current. Pearson [28] and Spearman [29] correlation analysis methods are utilized to evaluate the correlation between the two discharge parameters, as shown in **Table I**. The Pearson correlation coefficient represents the linear correlation between two parameters, and Spearman correlation coefficient represents the rank correlation. The longitudinal average light intensity integral has been proven to be significantly correlated with the discharge current during the transient discharge process. A remarkably strong correlation is observed during the streamer discharge period (0.3-0.92 μs). Throughout the discharge process, the rank correlation remains strong, but the linear correlation diminishes.

TABLE I

CORRELATION COEFFICIENT BETWEEN DISCHARGE

CURRENT AND AVERAGE LIGHT INTENSITY INTEGRAL IN DIFFERENT TIME RANGES

Time ranges (μs)	Pearson correlation coefficient	Spearman correlation coefficient
0.3-0.92	0.93	0.91
0.3-1.77	0.90	0.91
0.3-2.53	0.82	0.96
0.3-3.38	0.88	0.97

The relationships between the average light intensity integral (I) and discharge current (i) in the discharge images of the first and the second groups of experiments are shown in **Fig. 7**.

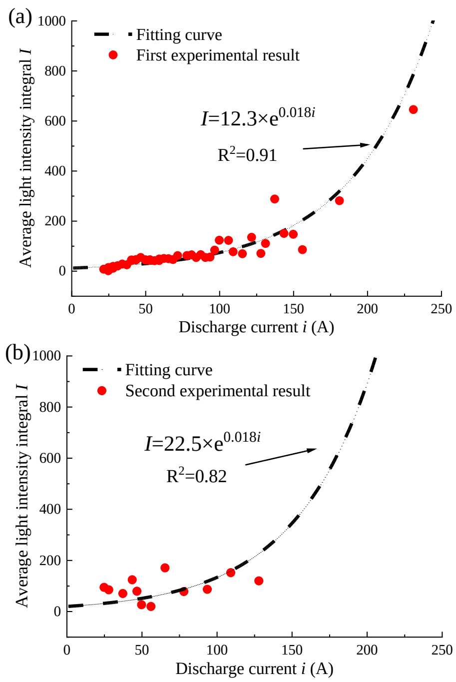

Fig. 7. Relationship between the average light intensity integral in discharge images and current. (a) The first group of experiments. (b) The second group of experiments. The fitting function and corresponding fitting goodness are given. *I* is the average intensity integral of the transient discharge image with 10 ns exposure time. *i* is the transient current at the time of shooting the image due to the extremely short exposure time.

There is a good nonlinear functional relationship between the two-dimensional discharge intensity image and the current in the first group of experiments. It can be represented by the exponential relationship ($I = ke^{ni}$) with a fitting goodness R^2 of 0.91. I is the average intensity integral of the transient discharge image with 10 ns exposure time, i is the transient current, k and n are the coefficients. When the derived relationship function is used to describe the results in the second group of experiments, the fitting goodness is 0.82 with the same coefficient n. The main difference between the two sets of experiments is the different shooting distances. The light intensity of discharge images captured at different shooting positions varies due to the influence of shooting distance on the amount of light entering the EMICCD. Therefore, it can be inferred that the coefficient k in the exponential function may be related to the measurement condition. And the coefficient n may be related to the discharge condition (such as electrode structure, air gap distance, voltage wave).

To further verify the applicability of the empirical formula, a validated experiment under the same discharge condition was conducted. In this experiment, each image in this experiment was captured at the same moment, but with varying exposure times (ranging from 50 ns to 2000 ns). The shooting distance was about 16 m. The cumulative impact of image light intensity could not be disregarded when studying their correlation. So the corresponding discharge current was the integrated current during the image exposure time. As shown in the **Fig. 8** (38 valid images), there is still a correlation between the integral of image light intensity and the corresponding current in time, which can be described by an exponential formula with the fitting goodness of 0.93. The coefficient n in this exponential formula matches exactly with the previous two sets of data, confirming the accuracy of the relationship formula and the validity of the coefficient analysis.

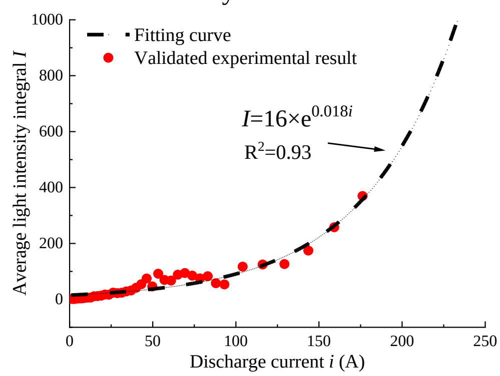

Fig. 8. The validation of the relationship between the average light intensity integral in discharge images and current. The fitting function and corresponding fitting goodness is given. *I* is the average intensity integral of the discharge image with different exposure time. *i* is the current integral within the exposure time range of the corresponding image.

V. Discussion

The qualitative relationship between the average light intensity integral of discharge images and current could be illustrated by the nonlinear exponential functions between the two discharge parameters. This exponential expression could be explained from two aspects. On the one hand, light intensity I is formed by photons generated during the discharge ionization process and related to the degree of ionization (characterized by the ionization coefficient). Collision ionization and photoionization are both proportional to the collision ionization coefficient [30, 31], and collision ionization coefficient is exponentially related to the electric field E. Meanwhile, thermoelectric ionization coefficient is exponentially related to the electric potential V. The electric field E and the electric potential V are proportional to the current i in long gap discharge [32, 33]. Therefore, it can be inferred that the relationship between the light intensity and discharge current is in exponential form. On the other hand, the current is formed by the movement of some free electrons formed by ionization, while light intensity is generated by all ionization processes. In the streamer stage, particularly with collision ionization, the rise in discharge light intensity is proportional to the increase in current. During the leader stage involving various ionization processes (especially thermoelectric ionization), strong multiple ionization leads to a greater increase in discharge light intensity than the increase in current. So, throughout the discharge process, the light intensity grows exponentially as the current increases.

There are limitations in this paper. First, the method of shooting one image per discharge results in dispersion in the image data, especially during the leader development process. The continuity of light intensity image changes in the leader stage is significantly worse than that during the streamer stage. Second, the average light intensity integral-current relationship and its empirical formula were validated under the same discharge conditions. The impact of various discharge conditions on the relationship between image light intensity and current has yet to be addressed. Third, a theoretical analysis of the empirical formula has been conducted, but due to the complexity of the whole long gap discharge process, the accurate physical formula needs further research.

Deep discussion on the correlation between image features and current under different exposure times, as well as the applicability of formulas and the variation characteristics of conditional coefficients under different experimental conditions, should be performed to derive more accurate physical formulas. In addition, the spatial charge characteristics of the discharge process can also be analyzed by combining current and image characteristics.

VI. Conclusion

Based on the 1m rod-plate gap discharge experiment platform under positive lightning impulse, this research measures the two-dimensional light intensity image with nanosecond scale exposure time, the discharge voltage, and the current. By analyzing the characteristics of light intensity images and the physical mechanism, the correlation between the average light intensity integral in the longitudinal direction and the discharge current is established. The empirical formula is suggested and discussed accordingly. The discharge image features mining and the relationship analysis with discharge current can achieve a description of discharge status and characteristics, and provide new ideas for the study of discharge space charge distribution and current monitoring methods.

Acknowledgment

The research is supported by Guangzhou Science and Technology Plan (2023A04J0293), and National Engineering Research Center of UHV Technology and Novel Electrical Equipment Basis (15000020220301003GY00020). The authors gratefully acknowledge Dr. Xiangen Zhao’s help to discharge experiments and all the members involved in the project.

References

[1] D. T. Markus and T. S. Lee, "A method of direct corona imaging on a dielectric transparency," *IEEE Transactions on Industry Applications,* vol. 32, no. 4, pp. 832-836, 1996, doi: 10.1109/28.511639.

[2] K. H. Schneider, "Positive Discharges in Long Air Gaps at Les Renardieres - 1975 Results and Conclusions," 1977.

[3] T. Suzuki and K. Miyake, "Breakdown process of long air gaps with positive switching impulses," *IEEE Transactions on Power Apparatus and Systems*, vol. 94, no. 3, pp. 1021-1033, 1975, doi: 10.1109/T-PAS.1975.31936.

[4] Z. Guo, Q. Ye, Y. Wang, Z. Yuan, and M. Wang, "Colorimetric Method for Discharge Status Diagnostics Based on Optical Spectroscopy and Digital Images," *IEEE Sensors Journal*, vol. 20, no. 16, pp. 9427-9436, 2020, doi: 10.1109/JSEN.2020.2988932.

[5] E. G. d. Costa, T. V. Ferreira, M. G. G. Neri, I. B. Queiroz, and A. D. Germano, "Characterization of polymeric insulators using thermal and UV imaging under laboratory conditions," *IEEE Transactions on Dielectrics and Electrical Insulation,* vol. 16, no. 4, pp. 985-992, 2009, doi: 10.1109/TDEI.2009.5211844.

[6] Z. Zhao, G. Xu, and Y. Qi, "Representation of binary feature pooling for detection of insulator strings in infrared images," *IEEE Transactions on Dielectrics and Electrical Insulation,* vol. 23, no. 5, pp. 2858-2866, 2016, doi: 10.1109/TDEI.2016.7736846.

[7] R. Ono and T. Oda, "Visualization of Streamer Channels and Shock Waves Generated by Positive Pulsed Corona Discharge Using Laser Schlieren Method," *Japanese Journal of Applied Physics*, vol. 43, no. 1R, p. 321, 2004/01/13 2004, doi: 10.1143/JJAP.43.321.

[8] P. Radhakrishnan, B. S. D. Sagar, and B. Venkatesh, "Morphological image analysis of transmission systems," *IEEE Transactions on Power Delivery,* vol. 20, no. 1, pp. 219-223, 2005, doi: 10.1109/TPWRD.2004.839213.

[9] M. Šimek, P. F. Ambrico, and V. Prukner, "ICCD microscopic imaging of a single micro-discharge in surface coplanar DBD geometry: determination of the luminous diameter of N2 and Ar streamers," *Plasma Sources Science and Technology,* vol. 20, no. 2, p. 025010, 2011/03/21 2011, doi: 10.1088/0963-0252/20/2/025010.

[10] S. Yu, T. Yao, and B. Yuan, "An ICCD camera-based time-domain ultrasound-switchable fluorescence imaging system," *Sci Rep,* vol. 9, no. 1, p. 10552, Jul 22 2019, doi: 10.1038/s41598-019-47156-x.

[11] A. D. Campiglia, S. Yu, A. J. Bystol, and H. Wang, "Measuring scatter with a cryogenic probe and an ICCD camera: recording absorption spectra in Shpol'skii matrixes and fluorescence quantum yields in glassy solvents," *Anal Chem,* vol. 79, no. 4, pp. 1682-9, Feb 15 2007, doi: 10.1021/ac061914s.

[12] M. Šimek, B. Pongrác, V. Babický, M. Člupek, and P. Lukeš, "Luminous phase of nanosecond discharge in deionized water: morphology, propagation velocity and optical emission," *Plasma Sources Science and Technology*, vol. 26, no. 7, p. 07LT01, 2017/06/26 2017, doi: 10.1088/1361-6595/aa758d.

[13] R. Zeng and S. Chen, "The dynamic velocity of long positive streamers observed using a multi-frame ICCD camera in a 57 cm air gap," *Journal of Physics D: Applied Physics*, vol. 46, no. 48, p. 485201, 2013/11/06 2013, doi: 10.1088/0022-3727/46/48/485201.

[14] P. Kochkin, A. P. J. van Deursen, and U. Ebert, "Experimental study on hard X-rays emitted from metre-scale negative discharges in air," *Journal of Physics D Applied Physics*, vol. 48, p. 025205, 12/16 2014, doi: 10.1088/0022-3727/48/2/025205.

[15] P. Kochkin, N. Lehtinen, A. P. J. van Deursen, and N. Ostgaard, "Pilot system development in metre-scale laboratory discharge," *Journal of Physics D Applied Physics*, vol. 49, p. 425203, 09/22 2016, doi: 10.1088/0022-3727/49/42/425203.

[16] A. Shirvani, W. Schufft, H. P. Pampel, and U. Schmidt, "Spatial-temporal investigation of breakdown of long air gaps by lightning voltages up to 2.4 MV," in *2013 IEEE Electrical Insulation Conference (EIC)*, 2-5 June 2013 2013, pp. 351-355, doi: 10.1109/EIC.2013.6554265.

[17] A. Shirvani Boroujeni, "Ein Beitrag zum Entladungsverhalten langer Luftfunkenstrecken bei Blitzspannung," Universitätsverlag Chemnitz, Chemnitz, 2015. [Online]. Available: http://nbn-resolving.de/urn:nbn:de:bsz:ch1-qucosa-158163.

[18] Z. Feng, "Research and Application of Image Feature Learning and Classification Methods Based on Deep Learning ", South China University of Technology 2017.

[19] Y. Yue and J. He, "Digital time-resolved optical measurement of discharge currents in long air gaps," *Review of Scientific Instruments*, vol. 84, no. 8, 2013, doi: 10.1063/1.4817208.

[20] X. Zhao *et al.*, "On the Velocity-Current Relation of Positive Leader Discharges," *Geophysical Research Letters*, vol. 46, no. 1, pp. 512-518, 2019, doi: https://doi.org/10.1029/2018GL081022.

[21] A. Gürlek, "Breakdown process on rod–rod air gap under oscillating lightning impulse voltage," *High Voltage*, https://doi.org/10.1049/hve.2019.0281 vol. 5, no. 3, pp. 319-326, 2020/06/01 2020, doi: https://doi.org/10.1049/hve.2019.0281.

[22] Y. Han *et al.*, "Study on Influencing Factors of Insulators Flashover Characteristics on the 110 kV True Tower Under the Lightning Impulse," *IEEE Access*, vol. 6, pp. 66536-66544, 2018, doi: 10.1109/ACCESS.2018.2878274.

[23] X. Zhao *et al.*, "Breakdown Characteristics of a 220-kV Composite Insulator String Under Short Tail Lightning Impulses Based on the Discharge Current and Images," *IEEE Transactions on Power Delivery*, vol. 33, no. 6, pp. 3211-3217, 2018, doi: 10.1109/TPWRD.2018.2874701.

[24] Y. Zhang *et al.*, "Study on Spatial-Temporal Distribution Characteristics of the Discharge Process in a 1 m Rod-Plate Gap Under Different Polarity Lightning Impulses," *IEEE Access*, vol. 7, pp. 111396-111410, 2019, doi: 10.1109/ACCESS.2019.2934406.

[25] *High-voltage Test Techniques-Part 1: General definitions and test requirements. Standard IEC 60060-1*, I. E. C. (IEC), 1989.

[26] *High-voltage test techniques-Part 2: Measuring systems. Standard IEC60060-2*, I. E. C. (IEC), 2010.

[27] P. Sylvain, K. Pierre, T. Jack, and D. Frédo, *Bilateral Filtering: Theory and Applications*. now, 2009, p. 1.

[28] A. H. Pripp, "[Pearson's or Spearman's correlation coefficients]," *Tidsskr Nor Laegeforen*, vol. 138, no. 8, May 8 2018, doi: 10.4045/tidsskr.18.0042. Pearsons eller Spearmans korrelasjonskoeffisienter.

[29] P. Sedgwick, "Spearman's rank correlation coefficient," *BMJ*, vol. 349, p. g7327, Nov 28 2014, doi: 10.1136/bmj.g7327.

[30] R. Morrow and J. J. Lowke, "Streamer propagation in air," *Journal of Physics D: Applied Physics*, vol. 30, no. 4, p. 614, 1997/02/21 1997, doi: 10.1088/0022-3727/30/4/017.

[31] Z. Yun, Z. Rong, Y. Xue-chang, Z. Bo, and H. Jin-liang, "Study on Photoionization Produced by Discharge in Atmospheric Air by Numerical Method," *Proceedings of the CSEE*, vol. 29, no. 04, pp. 110-116, 2009.

[32] G. I., "The mechanism of the long spark formation," *Journal De Physique*, 1979.

[33] N. Sato, "Discharge current induced by the motion of charged particles," *Journal of Physics D: Applied Physics*, vol. 13, no. 1, p. L3, 1980/01/14 1980, doi: 10.1088/0022-3727/13/1/002.

YAQI ZHANG, was born in Hunan province, China, in 1992. She received a B.Sc. degree in Changsha University of Science and Technology, China, in 2015. She received a Ph.D. degree at the School of electric power, South China University of Technology.

She is a lecturer at Guangdong Normal University of Technology now. And her research focuses on long gap discharge, lightning protection, and big data mining.